

## Practical guidelines for implementing adaptive optics in fluorescence microscopy

Wilding, Dean; Pozzi, Paolo; Soloviev, Oleg; Vdovin, Gleb; Verhaegen, Michel

**DOI**

[10.1117/12.2287647](https://doi.org/10.1117/12.2287647)

**Publication date**

2018

**Document Version**

Final published version

**Published in**

Proceedings of SPIE

**Citation (APA)**

Wilding, D., Pozzi, P., Soloviev, O., Vdovin, G., & Verhaegen, M. (2018). Practical guidelines for implementing adaptive optics in fluorescence microscopy. In T. G. Bifano, J. Kubby, & S. Gigan (Eds.), *Proceedings of SPIE: Adaptive Optics and Wavefront Control for Biological Systems IV* (Vol. 10502). [105021F] (Proceedings of SPIE; Vol. 10502). SPIE. <https://doi.org/10.1117/12.2287647>

**Important note**

To cite this publication, please use the final published version (if applicable).  
Please check the document version above.

**Copyright**

Other than for strictly personal use, it is not permitted to download, forward or distribute the text or part of it, without the consent of the author(s) and/or copyright holder(s), unless the work is under an open content license such as Creative Commons.

**Takedown policy**

Please contact us and provide details if you believe this document breaches copyrights.  
We will remove access to the work immediately and investigate your claim.

# PROCEEDINGS OF SPIE

[SPIDigitalLibrary.org/conference-proceedings-of-spie](https://spiedigitallibrary.org/conference-proceedings-of-spie)

## Practical guidelines for implementing adaptive optics in fluorescence microscopy

Dean Wilding, Paolo Pozzi, Oleg Soloviev, Gleb Vdovin, Michel Verhaegen

Dean Wilding, Paolo Pozzi, Oleg Soloviev, Gleb Vdovin, Michel Verhaegen, "Practical guidelines for implementing adaptive optics in fluorescence microscopy," Proc. SPIE 10502, Adaptive Optics and Wavefront Control for Biological Systems IV, 105021F (23 February 2018); doi: 10.1117/12.2287647

**SPIE.**

Event: SPIE BiOS, 2018, San Francisco, California, United States

# Practical guidelines for implementing adaptive optics in fluorescence microscopy

Dean Wilding<sup>a,†</sup>, Paolo Pozzi<sup>a,†</sup>, Oleg Soloviev<sup>a,b,c</sup>, Gleb Vdovin<sup>a,b,c</sup>, and Michel Verhaegen<sup>a</sup>

<sup>a</sup>Delft Center for Systems and Control, TU Delft, Mekelweg 2, 2628 CD Delft, The Netherlands

<sup>b</sup>Flexible Optical B.V., Polakweg 10-11, 2288 GG Rijswijk, The Netherlands

<sup>c</sup>ITMO University, Kronverksky 49, 197101 St Petersburg, Russian Federation

## ABSTRACT

In life sciences, interest in the microscopic imaging of increasingly complex three dimensional samples, such as cell spheroids, zebrafish embryos, and in vivo applications in small animals, is growing quickly. Due to the increasing complexity of samples, more and more life scientists are considering the implementation of adaptive optics in their experimental setups. While several approaches to adaptive optics in microscopy have been reported, it is often difficult and confusing for the microscopist to choose from the array of techniques and equipment. In this poster presentation we offer a small guide to adaptive optics providing general guidelines for successful adaptive optics implementation.

**Keywords:** Adaptive optics, fluorescence microscopy, wavefront sensing

## 1. INTRODUCTION — THE BASICS

The goal of this paper is to inform how to practically apply adaptive optics (AO) in fluorescence microscopy setups. As a practical guide, it shall be assumed that the physical understanding of microscopy systems is a given and instead will focus on directing how to implement a functional AO system that will improve the quality of images acquired by the system. Given the scope of ‘fluorescence microscopy’ it is obvious that it is not possible to go into all the details of how this may be achieved in every modality, but a helpful outline of the principles for the major groups of scanning and wide-field microscopes will be attempted.

To begin, it is useful to understand that the source of aberrations in fluorescence microscopy is the inhomogeneous distribution of refractive index in biological tissues — if system aberrations are neglected. It was understood from the beginning of microscopy that one could not look inside biological tissues very easily. The approach to this in the past was to use a microtome to cut the sample into thin quasi two-dimensional slices and build up a three-dimensional picture. Optical sectioning with confocal scanning systems or light-sheet<sup>1,2</sup> approaches has the same underlying principle except it uses light to achieve the same sectioning effect. The problem then is two-fold, the light used for sectioning is affected by the very same inhomogeneity that plagues the signal one is trying to acquire. Both need to be considered in an AO system.

In many microscopes the excitation and the illumination pass through the same aberration and therefore, a single adaptive optical element (AOE) can be used for *isoplanatic* correction, i.e. in a single point of the field-of-view (FOV). In other microscopy systems, a correction is required for the illumination and fluorescence independently meaning two AOE's are necessary. Furthermore, most aberrations introduced in microscope are *anisoplanatic*, meaning that a different correction for different areas of the FOV is also needed. With that said, there is often an average or global *isoplanatic* correction that will improve the image quality regardless of the *anisoplanatic* nature of the aberrations.

In Fig. 1 a schematic of this situation is shown. The light from two points in the sample is shown travelling from the source to the microscope objective. The light from the two sources travel through two distinct optical

---

Further author information: (Send correspondence to D.W. or P.P.)

D.W.: E-mail: d.wilding@tudelft.nl, Telephone: +31 15 278 1758; P.P.: E-mail: p.pozzi@tudelft.nl, Telephone: +31 15 278 1758. † D.W. & P.P. contributed equally to this manuscript.

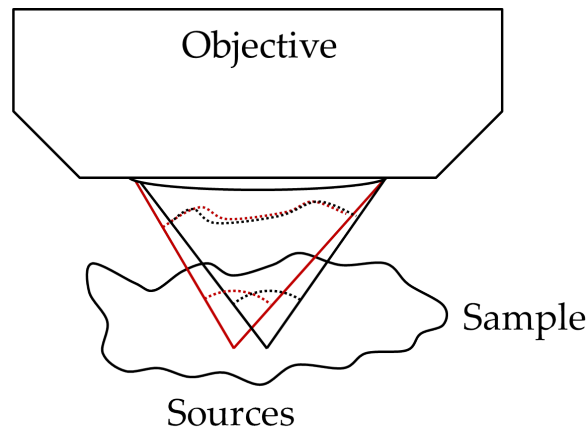


Figure 1. The source of aberrations in fluorescence microscopy comes from the inhomogeneous refractive index of biological tissues. Light from two different sources in the sample will travel through two different optical path lengths and thereby acquiring different phase delays.

paths and acquires two different phase aberrations. These would need two different corrections to be applied to the AOE in order to correct them perfectly.

The light from both these sources has maximum overlap in the pupil of the optical system. At this point, light from every point in the field of view is present over the whole surface of the corrector. This means that, if one applies a single correction in the pupil-plane it will affect all points in the field-of-view, this will result in some areas of the image improving and some areas degrading (depending on the particular aberration). For the reasons of universal effect most adaptive optics systems work by having their corrector and sensor in this pupil-plane.

The crucial point of understanding is that the correction required in biological samples is three-dimensional because the aberration is three-dimensional. It is impossible with a single plane corrector to achieve correction throughout the sample in one shot. For the purpose of extending the correction, multi-conjugate systems are being developed to provide a correction that more closely approximates the phase aberration present.<sup>3</sup>

Nevertheless, with a two-dimensional corrector in the pupil-plane of an optical system many things can still be done. AO as already touched upon has essentially three parts that must be considered. The first is the *sensing* of the wavefront aberration,<sup>4,5</sup> the second is the *corrector*,<sup>6,7</sup> and the final piece of the puzzle is the *controller*.<sup>8</sup>

## 2. WAVEFRONT SENSING

There are broadly two types of wavefront sensing that can be chosen: one in the pupil and one in the focal-plane of the system. In the majority of cases the choice will be determined by both one's available hardware budget and the modality of the microscope. Focal-plane sensing is more common in fluorescence microscopy since they can work at lower signal-levels, however, it is possible to apply pupil-plane sensors to fluorescence microscopy if one has the right budget, application and will-power.

The big difference between the two is that a focal-plane sensor uses the data directly from the imaging sensor, i.e. a scientific camera, photo-diode, etc. and only requires the addition of the corrector in the setup. Whereas, the pupil-plane sensor such as the Shack-Hartmann sensor<sup>9</sup> works by using a lenslet array in a secondary optical path and measures the displacement of an array of focal spots. The Shack-Hartmann is the only pupil-plane sensor that shall be treated in detail in this article, however, others exist such as the Partitioned Aperture Wavefront (PAW) sensor<sup>10</sup> and the pyramid sensor.<sup>11</sup>

### 2.1 The Focal-Plane Wavefront Sensor

Aberration correction based on a focal-plane wavefront sensor (FP-WFS) is generally performed by using the information from the microscope images themselves to estimate the optimal correction to apply on the AOE. All

that is necessary for realizing a FP-WFS system is the inclusion of the corrector normally in the pupil-plane of the system (possibly in other places too), which is usually done through a 4-f telescope. This is schematically shown in Fig.2. From an imaging point-of-view, the great advantage of this sensor is that no light is subtracted from the

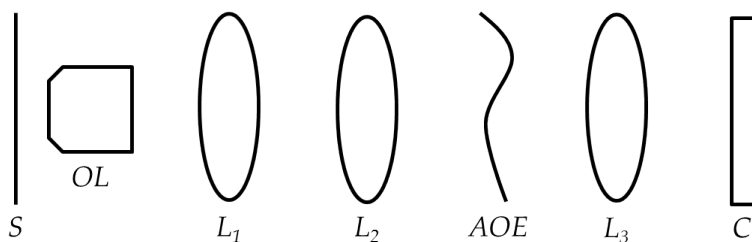


Figure 2. Focal-plane wavefront sensing setup.

imaging system in order to perform aberration correction. However, since the relationship between aberrations and image quality is non-linear, indirectly sensing the wavefront requires the acquisition of a substantial amount of images. While the wavefront can be elucidated by a pupil-plane wavefront sensor in 1-10 frames, it will take at least an order of magnitude more to acquire the same information with a FP-WFS.

The relationship between the phase in the pupil  $\phi$ , where the corrector is, and the intensity in the image plane  $i$ , where the sensor is, in the case of an isoplanatic aberration for incoherent imaging is modelled by:

$$i = |\mathcal{F}\{A \exp(j\phi)\}|^2 * o, \quad (1)$$

where  $o$  represents the fluorophore distribution, which for the analysis here can be a point-source  $\delta$ -function. The shape of the aperture is given by the function  $A$ . A corrector can introduce a change to the phase in the pupil such that it becomes  $(\phi + \varphi)$  and a metric function  $\sigma(i(\varphi))$  defining the quality or “goodness” of an image can be maximised:

$$\max_{\varphi} \sigma(i(\varphi)) \text{ or } \max_{\varphi} \sigma(|\mathcal{F}\{A \exp(j(\phi + \varphi))\}|^2 * o). \quad (2)$$

In order to maximise the metric, an optimisation algorithm must be employed (see Section 4), however, some information about the metrics is required at this point. If one is dealing with a point-source, this is “quite simple”. Maximisation of the brightest point, the second central moment of the spot, the image standard deviation or the spatial frequency content will all yield an optimisation that converges to the diffraction-limited spot. Depending on the order of the corrector, the length of time taken is dependent on the sensitivity of the metric and how many local maxima it has and how deep they are. The great benefit that one has with a point-source is that the optimal image is known, from basic optics theory, to be the Airy pattern for a circular aperture.

On the other hand, if one has an extended source the problem is much more difficult. It is not known *a priori* what the best image is. A good approach in this case is to include some *a priori* information, for example, if it is possible to encode a particular spatial frequency into the image by modulating the illumination. In this case, maximising this particular spatial frequency is akin to reducing the aberration. If modulation of the illumination is not possible then maximisation of the power spectrum of the image within a given radius in the Fourier domain is an alternative and a somewhat robust methodology.<sup>12</sup> The success or failure of these optimisation procedures is very dependent on the amount of out-of-focus fluorescence and the photo-bleaching rate.

A drawback is that most metrics are indirectly dependent on the amount of signal. As the procedure can take many frames  $> 100$ , it is not uncommon that the amount of light collected from the fluorophores decreases over time. This can lead to frames later in the acquisition being scored lower or higher than those at the start, leading to a misleading quantification — especially if the approach is model-based (see Section 4). The summation of out-of-focus fluorescence can also lead to false-positive optimisation.

Furthermore, it is often necessary to exclude displacement modes (i.e. tip, tilt and defocus) from one’s optimisation space since instead of changing the image quality, they move the FOV through the sample, and the correction procedure would therefore just find the FOV where the metric is maximized, not the maximum of the desired FOV. These considerations makes wavefront sensing with extended objects in wide-field microscopy problematic.

## 2.2 The Pupil-Plane Wavefront Sensor

The pupil-plane wavefront sensor (PP-WFS), specifically here the Shack-Hartmann, requires loss of photons or the use of a second fluorophore at a different wavelength. It also requires the use of point-sources, in microscopy this implies the introduction of non-biological guides in the form of beads to act as localised sources of aberration information.<sup>5</sup> The downside of this is obviously the introduction of a foreign agent is going to activate an immune response *in vivo* and may effect the biology of what is being studied.

The PP-WFS configuration is shown in Fig. 3 and as can be observed it is practically more difficult to implement than the FP-WFS c.f. Fig. 2. For standard operation, the PP-WFS must be conjugated to the corrector and the pupil-plane of the objective giving a linear relationship between the corrector inputs and the measured phase. (The procedure for this will be described in the subsequent Section 3.) The ratio of the beam splitter must be chosen to ensure the correct amount of light for imaging and for wavefront sensing if using one wavelength. The lenslet array (LA) pitch  $p$  (the distance between lenses) and its focal length ( $f_A$ ) affect the resolution and the amplitude of the phase aberration that the sensor can detect. It is necessary to have a rough estimate of what is required before purchasing one of these. As a guide, the maximum phase gradient that can be measured by a particular Shack-Hartmann is given by:

$$\langle \nabla \phi \rangle_{\max} \approx \frac{\pi p^2}{2\lambda f_A}. \quad (3)$$

from which it can be deduced that the larger the value of  $f_A$  the smaller the displacement for the same phase gradient. It must also be considered that the pitch defines the sampling resolution of the pupil. In this case, a large pitch with a short focal length allows the measurement of large low order aberrations. From a pure adaptive optics perspective, unless the entire system is designed *ad hoc*, the rule-of-thumb in the selection of a sensor is using a number of sub-apertures equal to around three times the number of corrector actuators. Additional factors, however, must be considered based on the nature of aberrations. A small pitch with large focal length allows the measurement of smaller high order aberrations. Moreover, the signal from the point source is split between sub-apertures, so the more lenslets the less light per sub-aperture, therefore, the signal-to-noise ratio is lower and the computational complexity increases — not a optimal trade-off.

Another important metric is the dynamic range of the total lenslet array and this can be computed for a given aberration. For example, the total defocus stroke of the system with  $M \times M$  lenslets and normalised radius  $0 \leq \rho \leq 1$  may be approximated in the following way:

$$\begin{aligned} \phi_1 &= 2\pi \Delta \lambda_{\text{def}} \rho^2, \\ M \langle \nabla \phi \rangle_{\max} &= 4\pi \Delta \lambda_{\text{def}}, \\ \Delta \lambda_{\text{def}} &= \frac{M p^2}{8\lambda f_A}. \end{aligned} \quad (4)$$

A typical lenslet array could have  $p = 300\mu\text{m}$ ,  $f_A = 17.526\text{ mm}$ , and around  $M = 20 \times 20$  lenslets — this gives a  $\Delta \lambda_{\text{def}} \approx 26$  or 165 radians peak-to-valley. Other aberrations have a more complex spatial distribution and therefore, cannot necessarily be computed so easily.

The signal level, however, will be the biggest hindrance to successful operation. Each sub-aperture of the sensor consumes signal-to-noise ratio. The noise in the centroid measurements affects the ability to correctly identify the wavefront. This means it may be necessary to reduce the number of sub-apertures, in turn reducing the spatial resolution and dynamic range of the sensor, in order to have a working system. Not everything that is wished for may be possible.

For example, it is theoretically possible to have an AO system that could continually correct for every position of the scanner in a confocal scanning or two-photon system. The problem here is that sensor would have to be able to detect light at low signal-to-noise ratios and high-speeds that are out of reach for even the best current EMCCD cameras. As a compromise with the sensor the signal may be integrated over the whole period of a single frame, the de-scanned light will be averaged over the sensor giving the average aberration over the field-of-view instead — not as good correction but better than nothing.

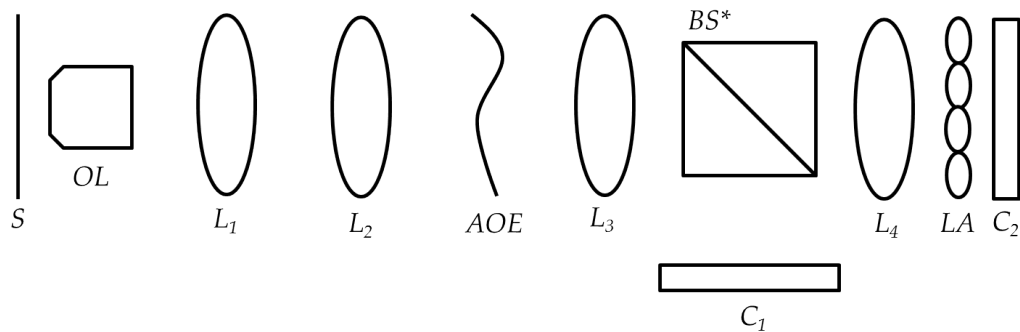


Figure 3. pupil-plane wavefront sensing setup with a Shack-Hartmann sensor. \*The beam-splitter (BS) here can be a dichroic beam splitter.

As an aside, the PP-WFS can also be used on wide-field images, only if a field stop or “guide stars” are used. In this case, the fluorophore needs to be very bright and the noise reduced as much as possible. Another approach is to use the multiple images of the sample and use cross-correlation to detect local shifts in the images. This once again requires a very good signal-to-noise ratio for successful application. To conclude, for wide-field imaging especially and fluorescence microscopy in general it is not usually possible to employ a pupil-plane sensor.

### 3. WAVEFRONT CORRECTION

In order to perform correction of aberrations, a multi-actuator, bi-dimensional phase modulator is generally placed in a pupil-plane of the system. With the exception of deformable lenses,<sup>13</sup> and transmissive liquid crystal spatial light modulators, most phase modulators are reflective. Since the pupil-plane of most microscope objective is physically inside the objective itself, a secondary pupil-plane must be created through a 4-f telescope. This is illustrated in Fig. 4, where the AOE is placed in plane  $P'$ .

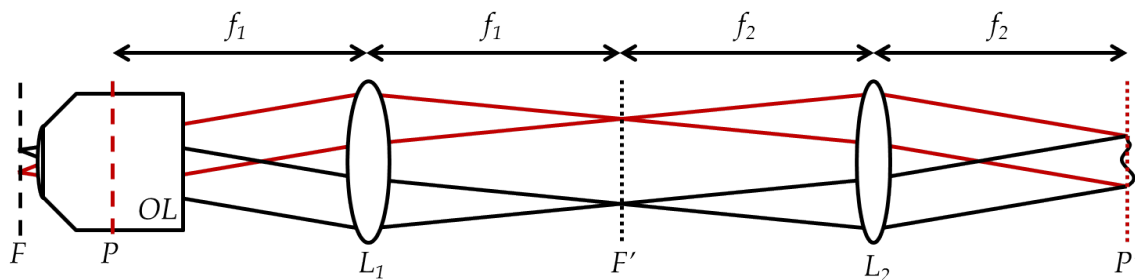


Figure 4. Where to place the corrector in a pupil-plane configuration, in  $P'$  that is conjugated via a 4-f system to the objective pupil-plane  $P$ .

The size of the back aperture plane of the objective should be calculated from its magnification and numerical aperture, and the focal lengths of the telescope must be correctly estimated so that the image of the objective’s pupil-plane at the AOE location is equal to the size of the AOE. In general, it is good practice to design the optical system with a specific microscope objective and AOE in mind, as the use of a different objective, or an AOE of different size, would require a re-design of the telescope conjugating the two planes.

In the case of deformable mirrors (DM), the main actuator technologies commercially available are piezoelectric, electrostatic membrane, voice coil and micro-machined silicon. A notable alternative is constituted by liquid crystal spatial light modulators, which only work on coherent monochromatic light, and are therefore only suitable for multi-photon laser scanning microscopy.

Each technology represents a trade-off in the main technical specifications, namely: response time, actuator number, correction stroke, repeatability of the correction, and cost. A summary of performance comparison is

Table 1. Information on different types of deformable mirrors.

Type	Response time	Stroke	Order	Hysteresis	Cost	Ideal Application
Piezo	***	**	*	*	\$	Closed-loop systems, model-free correction
Membrane	***	**	**	***	\$	Model-based correction, dynamic refocusing
Voice Coil	***	****	**	**	\$\$	Deep tissue isoplanatic correction
Micromachined	***	*	****	****	\$\$\$\$	Anisoplanatic & scattering compensation
LCD SLM	*	****	****	****	\$\$\$	Anisoplanatic & scattering compensation, beam-shaping
Adaptive Lens	**	*	*	*	\$\$	Low-order correction, modification of commercial setups

reported in Table 1. The reader should notice that no numbers are reported, as constant evolution of technology means the better products are often reported on the market. Even the comparison reported in the table could be very easily outdated on a short notice, so the authors still suggest, when choosing a modulator, to request quotes and data-sheets for a wide array of technologies before committing to one. What may work for one configuration and application does not make it a good fit for another application. The main features to look out for are:

**Response time** It is generally not considered as a critical parameter for microscopy, as the response time of most DMs (usually on the sub-millisecond scale) is much faster than the frame rate of any microscope, or any wavefront sensor operating in low light conditions. Spatial light modulators are a notable exception, as their refresh time can be as low as a few Hz, and may constitute a limit to the correction speed of the entire AO system.

**Number of actuators** It is a very sample specific parameter, as the amplitude and order of aberrations can vary wildly with the index of refraction distribution in a biological sample. It must be considered, however, that while a high order corrector with a high number of actuators can achieve correction in highly scattering materials,<sup>3</sup> the size of the field-of-view where the correction is valid decreases with the order of the aberration, so that special and more complex hardware and software configurations are needed to take full advantage of a high-order corrector. Moreover, higher numbers of actuators require longer optimisation procedures, or higher numbers of sub-apertures in wave-front sensors, therefore, reducing the usability of the microscope. It is, therefore, a generally good suggestion for a simple isoplanatic AO system to choose lower order correctors.

**Stroke** Another sample dependent parameter, however, an high stroke can be extremely helpful in some specific situations. Using dry objectives or oil immersion objectives, a severe spherical aberration will inevitably appear and increase linearly with sample depth, and can only be compensated with with very high stroke mirrors. Moreover, high stroke allows for additional refocusing or scanning capabilities.

**Repeatability** Piezoelectric actuators, and less noticeably voice coil actuators, are affected by hysteresis and creep, which may hinder the repeatability and stability of input response. While this is a generally negligible



problem if case of pupil-plane wavefront sensing and model-free optimisation methods, model-based optimisation applications can be greatly affected, so hysteresis-free modulators such as membrane mirrors are to be preferred.

## 4. CONTROLLERS

### 4.1 Introduction to Control

The purpose of a controller is to take the sensor measurements whether from the focal-plane or the pupil-plane and convert this into control inputs for the corrector. It is possible to do this in a number of ways and best method depends on the type of sensor and the application. This is summed up in Table 2.

There are two broad categories that one can chose for controlling an adaptive optics system. The first type is called *model-free* and the second category is *model-based*. From the names it is possible to imagine that the difference in these two is the explicit making of a model of the optical system. Model-free control can only really apply to the case of indirect sensing, it would be possible to apply this to a pupil-plane sensing but it is not immediate clear why one would want to do this. Since the purpose of using a wavefront sensor is so that there is a simple linear relationship between the correction phase and the measurement. This linear relationship allows the correction to be done very quickly and with *closed-loop* feedback.

### 4.2 Pupil-Plane Sensors

Whilst there are much more complex methods of control but the simplest approximates the relationship between the sensor and the corrector as being purely linear. This behaviour is contained in  $H$ , the influence matrix, and it is responsible for turning centroid displacements  $\mathbf{s}$  from a flat reference into actuators inputs  $\mathbf{u}$  for the AOE:

$$\mathbf{s} = H\mathbf{u} \quad (5)$$

The Shack-Hartmann sensor output is a vector of centroid displacements for a 2D array of focal points. It is possible to relate the average phase gradient  $\langle \nabla \phi \rangle_i$  in the  $i^{\text{th}}$  sub-aperture to the centroid displacement  $(\bar{x}_i, \bar{y}_i)$  of the focal spot in the sub-aperture by:

$$s_i = (\bar{x}_i, \bar{y}_i) \approx f_A \langle \nabla \phi \rangle_i = f_A \left( \left\langle \frac{\partial \phi}{\partial x} \right\rangle_{(x_i, y_i)}, \left\langle \frac{\partial \phi}{\partial y} \right\rangle_{(x_i, y_i)} \right). \quad (6)$$

To control the system, one needs to find first a flat reference input array,  $\mathbf{u}_0$ , through optimisation (see Section 4.3) and then one can calculate the matrix  $H$  relative to this flat wavefront position. The simplest way to do this is by measuring the response of the sensor to a perturbation of a single actuator, for example, actuator 1:

$$\mathbf{s}_1 = H \begin{pmatrix} 1 \\ 0 \\ \vdots \\ 0 \end{pmatrix} = \begin{pmatrix} H_{11} & 0 & \dots & 0 \\ H_{21} & 0 & \dots & 0 \\ \vdots & \vdots & \ddots & \vdots \\ H_{N1} & 0 & \dots & 0 \end{pmatrix}, \quad (7)$$

when repeated for all actuators this builds up a complete  $H$  matrix. To use for control, it needs to be inverted either using the Penrose-Morse pseudo-inverse or single value decomposition (SVD). In pseudo-inverse form it appears as the following:

$$\mathbf{u} = (H^\dagger H)^{-1} H^\dagger \mathbf{s} \quad (8)$$

For closed-loop operation, it is necessary to feedback a fraction of this ( $0 \leq \gamma \leq 1$ ) to the existing input signals in the following manner:

$$\mathbf{u}^{(k+1)} = \mathbf{u}^{(k)} - \gamma (H^\dagger H)^{-1} H^\dagger \mathbf{s}^{(k)}. \quad (9)$$

Table 2. Information on different types of AO control. The values in the Table are approximations based on current technological possibilities and will change over time.

Type	Speed	Aberration Size	Order	SNR
Model-free optimisation	$\mathcal{O}(10^2)$ s	$< 60\lambda$	$< 20$	$> 10$ dB
Model-based optimisation	$\mathcal{O}(10^1)$ s	$< 20\lambda$	$< 60$	$> 15$ dB
Wavefront Sensor	$\mathcal{O}(10^{-2})$ s	$< 40\lambda^*$	$< 60$	$> 10$ dB

\* The limit is on the phase gradient within a lenslet as discussed in Section 2.

### 4.3 Indirect Optimisation

Both optimisation techniques depend on the computation of a metric to quantify the quality of the image, as in Eq. (2). An optimisation algorithm is then used to find the maximum of this metric. This metric may be considered to form a multi-dimensional surface, where one is trying to find the highest peak. In Fig. 5 a landscape is shown in schematic form for two-dimensions. The type of algorithm, Fig. 5(a) showing a model-based approach and Fig. 5(b) showing the model-free approach determines the set of measurements at specific inputs that need to be measured to find the peak.

The figure has been intentionally drawn to show that there can be two types of metric shapes in general, those that are *convex* with respect to the degrees of freedom as in Fig. 5(a) or *non-convex* as in Fig. 5(b). Non-convexity implies that function does not have one unique maximum and it is possible to converge to a local maxima, that do not offer the globally best solution. Whereas, in convex optimisation if one converges to a maximum one can be certain that it is global.

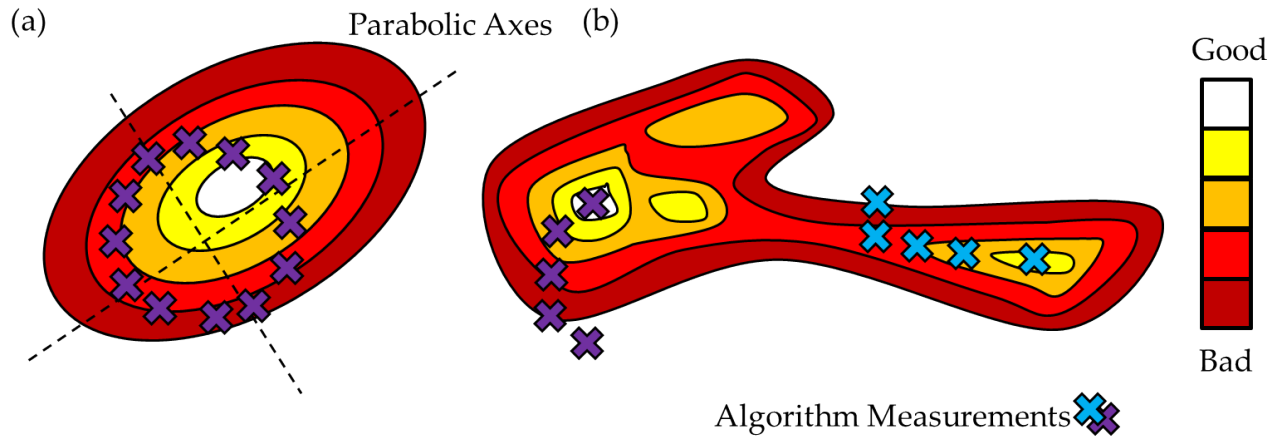


Figure 5. A sketch of difference between (a) model-based optimisation approach and (b) model-free optimisation approaches. In reality, this optimisation landscape is in many more dimensions and depending on the metric may have more or less local maxima.

#### 4.3.1 Model-free optimisation

Model-free control is usually performed with non-convex metrics, systems that are not well-defined, or have a low signal-to-noise ratio. It is an approach that is almost guaranteed to work to control an optical system. The method is slow, but it is robust and is able to operate with a low signal-to-noise ratio on a system that you do not know very much *a priori* about. As such, it is recommended to use this approach to test whether the combination of AOE and your application are compatible and then to progress to a more complex methodology.

**Metrics** The first and most crucial step is designing a metric to evaluate. As previously remarked upon, in wide-field microscopy the definition of such a metric is challenging and can be very sample dependent. Nevertheless, a examples of the broad spectrum of approaches is listed here:

- Brightness —  $\sum_{xy} i(x, y)$ .
- Sharpness —  $\sum_{xy} i(x, y)^2$ .
- Frequency content in an annulus  $\mathcal{R}$  —  $\sum_{\mathcal{R}} |\mathcal{F}\{i(x, y)\}|^2$ .
- Intensity gradient —  $\sum_{xy} |\nabla i(x, y)|^2$ .
- Second central moment —  $\sum_{xy} (x - \bar{x})^2 (y - \bar{y})^2 i(x, y)$

**Algorithms** The choice of algorithm is not as important as the metric, however, for a given application one may desire the measurements to progress in a particular manner — such as small incremental steps rather than large scans. An incomplete list is given here:

- *Coordinate Search (CS)* — sequentially scan through a range of aberration values along the degrees of freedom and find the maxima. Simple to implement and fairly robust, but can give a result that is not a true maximum.
- *Stochastic Gradient Descent/Ascent* — randomly perturb the aberration values by a small amount, if it gives a better value keep the perturbation, if not revert. Will converge to local maxima.
- *Gradient Descent/Ascent* — measure the multi-dimensional gradient of the metric then take a positive step in the steepest direction. This will quickly converge to a local maximum but can easily diverge in the presence of noise.
- *Second-order gradient methods, BFGS,<sup>14</sup> etc.* — these compute the Hessian to find extra information about the metric function. Faster than first-order methods but even more sensitive to noise. These work better with analytically evaluable functions and again these can diverge if the noise is too high.
- *Simplex* — measure the metric for a set of aberration values then compute the metric weighted centre-of-mass in the aberration coefficients space, next measure the metric at this new aberration values and replace the lowest metric value with the new measurement then repeat. Will converge to the closest local maximum, it is slower but less sensitive to noise than the gradient-based approaches.
- *Genetic algorithms, simulated annealing, etc.* — work by searching the space of possible aberration values for the most “fit” solution. These algorithms are for when one has a poor understanding or knowledge of the metric or system. They are almost certain to converge to the global maximum, but can take a very long time to get there.
- *DONE algorithm<sup>15</sup>* — an algorithm developed by one of the authors of this article, generating a dynamic model of the metric function as a series of cosine functions whose coefficients are determined by the available measurements of the metric. Each successive new measurement is performed close to the estimated minimum of the function, and added to the model. Slower in convergence than the gradient-based methods, but it is extremely robust to noise and can avoid local maxima. Careful hyper-parameters determination is required making it quasi-model-based.

### 4.3.2 Model-based optimisation

Model-based control requires the use of *a priori* information about the setup and the nature of light propagation through aberrations. This type of control imposes much more stringent conditions on the optical setup and is sensitive to anything that can change the model, such as misalignment or different sample types, etc.

In most model-based AO implementations in microscopy, the metric is assumed to be quadratic function of the correction inputs  $a$ :

$$M(\varphi) \approx M_0 - a^T \mathbf{B}a, \quad (10)$$

which is a system with  $N$  degrees of freedom (usually the number of actuators of the AOE), is determined by  $\mathcal{O}(N^2)$  parameters. It is possible to determine, usually through a lengthy calibration procedure, a specific aberration base for which the matrix  $B$  is diagonal, so that the function can be more easily expressed as:

$$M(\varphi) = M_0 + \sum_{n=1}^N b_n a_n^2. \quad (11)$$

In this case, the absolute minimum can be easily found, in low noise scenarios, with only  $2N+1$  measurements, by measuring the value of the metric with no correction applied, and sequentially for two additional values of each element of the aberration base. With this data the values of  $b_n$  can be easily identified, and the minimum location can be extrapolated.

This provides much faster convergence than any model-free method, reaching performances similar to those of a wavefront sensor based system. However, calibration of a base respecting the condition in Eq. (11) is non-trivial, and small misalignments of the system, or use of different samples can easily render the calibration ineffective, and severely affect the performances of the optimisation. A few examples may be found in the following articles:

1. Second central moment metric with Lukosz-Zernike (LZ) functions.<sup>16</sup>
2. Mean image intensity in two-photon microscopy with an orthogonalised base.<sup>17</sup>
3. Second central moment metric with gradient orthogonal functions.<sup>18</sup>

In summary, the advantage yielded by these techniques is that the speed at which correction may be done is increased over model-free approaches. The disadvantage of this approach is that the technique requires the metric function to have a known form, which can generally only be guaranteed over a small aberration range. If one wishes to apply this approach, one must find a good metric for one's imaging modality and quantify it analytically. From this model of the image formation process calculate a set of basis functions that are orthogonal with respect to this metric. In this way, within the scope of the model the metric function will be convex around the maximum of the function for small enough perturbations and correction can be done quickly.

## 5. CONCLUSIONS

It should be clear from the discussion in this paper that the choice of sensing, corrector and controller are dependent on one's application and the type of corrections one wishes to make. Before getting out the cheque book one needs to carefully determine what parameters are suitable to one's application.

If one is in the fortunate situation of having a scanning system with a high signal-to-noise ratio, a pupil-plane wavefront sensor will provide a fast and robust AO system that can be run in closed-loop. This type of system has been thoroughly researched and there are many different controllers that can be adapted for use in microscopy. In a wide-field system with a good signal to noise ratio, it could be possible to find an extended source wavefront sensor, however, this approach is much less refined and is more a research topic than a tool for improving your images.

In the vast majority of cases in fluorescence microscopy, therefore, indirect sensing will be used and the design of a suitable metric for one's application is an *essential* first step. From here one needs to decide if the signal-to-noise ratio of your images are good enough for the determination of a model. If so, a model-based

approach will provide a faster but less robust solution — the quality of the metric is a large factor in determining the success of the approach or not and is dependent on the modality. In the case of poor signal-to-noise and no *a priori* information a model-free focal-plane sensing system is the best choice, however, it can take a long time to converge to a solution and is not particularly suitable for light-sensitive samples that photo-bleach or die quickly.

To conclude, applying AO in microscopy is about understanding your needs, your resources, and finding the compromise that allows for some of the correction you want to see at an acceptable cost of those resources (money, photons, time, etc.).

## ACKNOWLEDGMENTS

The authors would like to acknowledge the technical contributions of W.J.M. van Geest and C.J. Slinkman. The authors are also thankful to Flexible Optical B.V. for their continued advice and support in their research. The research leading to these results has received funding from the European Research Council under the European Union's Seventh Framework Programme (FP7/2007-2013). ERC Grant Agreement No. 339681.

## REFERENCES

- [1] Voie, A., Burns, D., and Spelman, F., "Orthogonal-plane fluorescence optical sectioning: Three-dimensional imaging of macroscopic biological specimens," *Journal of microscopy* **170**(3), 229–236 (1993).
- [2] Huisken, J., Swoger, J., Del Bene, F., Wittbrodt, J., and Stelzer, E. H., "Optical sectioning deep inside live embryos by selective plane illumination microscopy," *Science* **305**(5686), 1007–1009 (2004).
- [3] Park, J.-H., Sun, W., and Cui, M., "High-resolution in vivo imaging of mouse brain through the intact skull," *Proceedings of the National Academy of Sciences* **112**(30), 9236–9241 (2015).
- [4] Wilding, D., Pozzi, P., Soloviev, O., Vdovin, G., and Verhaegen, M., "Adaptive illumination based on direct wavefront sensing in a light-sheet fluorescence microscope," *Optics express* **24**(22), 24896–24906 (2016).
- [5] Tao, X., Fernandez, B., Azucena, O., Fu, M., Garcia, D., Zuo, Y., Chen, D. C., and Kubby, J., "Adaptive optics confocal microscopy using direct wavefront sensing," *Optics letters* **36**(7), 1062–1064 (2011).
- [6] Vdovin, G. and Sarro, P., "Flexible mirror micromachined in silicon," *Applied optics* **34**(16), 2968–2972 (1995).
- [7] Bifano, T. G., Mali, R. K., Dorton, J. K., Perreault, J. A., Vandelli, N., Horenstein, M. N., and Castanon, D. A., "Continuous-membrane surface-micromachined silicon deformable mirror," *Optical Engineering* **36**(5), 1354–1361 (1997).
- [8] Booth, M. J., "Adaptive optics in microscopy," *Philosophical Transactions of the Royal Society of London A: Mathematical, Physical and Engineering Sciences* **365**(1861), 2829–2843 (2007).
- [9] Platt, B. C. and Shack, R., "History and principles of shack-hartmann wavefront sensing," *Journal of Refractive Surgery* **17**(5), S573–S577 (2001).
- [10] Li, J., Beaulieu, D. R., Paudel, H., Barankov, R., Bifano, T. G., and Mertz, J., "Conjugate adaptive optics in widefield microscopy with an extended-source wavefront sensor," *Optica* **2**(8), 682–688 (2015).
- [11] Ragazzoni, R., "Pupil plane wavefront sensing with an oscillating prism," *Journal of modern optics* **43**(2), 289–293 (1996).
- [12] Débarre, D., Booth, M. J., and Wilson, T., "Image based adaptive optics through optimisation of low spatial frequencies," *Optics Express* **15**(13), 8176–8190 (2007).
- [13] Bonora, S., Jian, Y., Zhang, P., Zam, A., Pugh, E. N., Zawadzki, R. J., and Sarunic, M. V., "Wavefront correction and high-resolution in vivo ophthalmic imaging with an objective integrated multi-actuator adaptive lens," *Optics express* **23**(17), 21931–21941 (2015).
- [14] Fletcher, R., [*Practical methods of optimization*], John Wiley & Sons (2013).
- [15] Blik, L., Verstraete, H. R., Verhaegen, M., and Wahls, S., "Online optimization with costly and noisy measurements using random fourier expansions," *IEEE transactions on neural networks and learning systems* (2017).
- [16] Booth, M. J., "Wavefront sensorless adaptive optics for large aberrations," *Optics letters* **32**(1), 5–7 (2007).

- [17] Débarre, D., Botcherby, E. J., Watanabe, T., Srinivas, S., Booth, M. J., and Wilson, T., “Image-based adaptive optics for two-photon microscopy,” *Optics letters* **34**(16), 2495–2497 (2009).
- [18] Pozzi, P., Wilding, D., Soloviev, O., Verstraete, H., Blik, L., Vdovin, G., and Verhaegen, M., “High speed wavefront sensorless aberration correction in digital micromirror based confocal microscopy,” *Optics Express* **25**(2), 949–959 (2017).